Optics Communications 412 (2018) 141–145

Contents lists available at ScienceDirect

Optics Communications

journal homepage: www.elsevier.com/locate/optcom

Control over high peak-power laser light and laser-driven X-rays

Baozhen Zhao, Sudeep Banerjee, Wenchao Yan, Ping Zhang, Jun Zhang, Grigory Golovin, Cheng Liu, Colton Fruhling, Daniel Haden, Shouyuan Chen, Donald Umstadter *

Department of Physics and Astronomy, University of Nebraska, 855 N 16th Street, Lincoln, NE 68588, USA

ARTICLE INFO

Keywords:
High-power laser control
Inverse Compton scattering
Ultra-high intensity control
Compton X-rays
Tunable dose

ABSTRACT

An optical system was demonstrated that enables continuous control over the peak power level of ultrashort duration laser light. The optical characteristics of amplified and compressed femtosecond-duration light from a chirped-pulse amplification laser are shown to remain invariant and maintain high-fidelity using this system. When the peak power was varied by an order-of-magnitude, up to its maximum attainable value, the phase, spectral bandwidth, polarization state, and focusability of the light remained constant. This capability led to precise control of the focused laser intensity and enabled a correspondingly high level of control over the power of an all-laser-driven Thomson X-ray light source.

1. Introduction

High-peak-power laser systems have undergone rapid progress recently, enabled by the development of various techniques including chirped pulse amplification (CPA) [1], optical parametric chirped pulse amplification (OPCPA) [2], and the availability of high quality large diameter amplifier gain media [3–5]. Based on these advances, several petawatt (PW) peak-power laser systems are now operational [6–8], and a number of multi-PW systems are under construction. In turn, these laser advances are facilitating rapid progress in research and development in the emerging area of high-field science, including fundamental studies of the interactions of light with matter at ultra-high intensity levels [9], as well as the development of ultra-high-gradient charged-particle accelerators [10,11], high-brightness X-ray light sources [12,13], and high-flux neutron sources [14,15].

Progress in high-field science and technology development depends not only on the ability to generate high peak-power laser light but also on the ability to focus that power to ultra-high intensity [16] and control the level of that intensity continuously [17]. For example, the signatures of nonlinear and quantum effects in high-field scattering experiments are found by identifying subtle correlations between the input laser intensity and the output X-ray and electron parameters [18]. Laser-driven electron and ion accelerators [19], as well as X-ray sources, are each optimized at specific and well-defined laser intensity levels.

Several techniques have been implemented to focus laser light of a given peak power to its highest intensity level. For instance, deformable mirrors with active feedback control loops are now used to correct any spatial phase imperfections in the laser beam that were acquired during amplification. In addition, to avoid additional phase distortions generated when high peak-power light propagates through refractive media, only reflective optics are used under vacuum after amplification and pulse compression. In prior work, all attenuation systems, designed to adjust the laser intensity level on target continuously, have invariably required the use of refractive optics. In this work, we present a simple and novel optical system that overcomes this problem. We show that it is able to attenuate the peak power of laser light in a continuous and controllable way while preserving spectral and spatial fidelity nearly ideally. The spectrum, spatial phase-front, and polarization of the attenuated pulses remain unchanged even as the peak laser power is varied—over a dynamic range that extends over an order-of-magnitude, up to the maximum attainable power level. Additionally, we showed the importance of this control over the laser intensity by demonstrating that it enables us to control the power of a recently developed laser-driven X-ray light source [13], which may prove to be useful for low-dose radiological applications.

Numerous methods are used to vary the energy of laser beams. The simplest and most common way is to place neutral density filters in the amplified beam, which only permits the variation of the energy in large discrete steps. For continuous variation of energy, a combination of a half-wave-plate (HWP) and polarizer is used. The use of such refractive optics is limited to low-power laser pulses due to B-integral effects and the low damage threshold of the associated optics. The output energy of a laser amplifier can also be varied by varying the energy of the seed

* Correspondence to: Behlen Laboratory, 500 Stadium Drive, Lincoln, NE 68588W, USA.
E-mail address: donald.umstadter@unl.edu (D. Umstadter).

https://doi.org/10.1016/j.optcom.2017.11.079
Received 22 June 2017; Received in revised form 7 November 2017; Accepted 28 November 2017
0030-4018/

or pump beam as well as by changing the timing between them [20]. In the latter scheme, the output energy is reduced by operating the amplifier away from its optimal point, resulting in large fluctuations of the laser output energy as well as a change in the temporal contrast. We previously implemented a device consisting of a zero-order half-wave plate (ZHWP) and broadband thin film polarizers (TFP) [21] used to control the output energy at the exit of the amplifier. This has been shown to have excellent characteristics with regard to precise control of the laser energy. However, the polarizers that are used require an incident angle of ~72° to support the laser spectrum and minimize dispersion [22]. This large angle of incidence leads to the requirement that the TFP be > 4 times the size of the incident beam. This requirement is not practical for PW-level laser systems, where the beam size can be 10 cm or even larger depending on the energy of the beam. The thickness needs to be small to keep B-integral induced distortion of the beam to a minimum. Such optics are expensive and difficult to manufacture.

Other methods exist to adjust the energy level of a high-power chirped-pulse-amplified laser, either during or after pulse compression. For example, clipping the spectrum between the two gratings in the pulse compressor will lower the energy but also lengthen the pulse duration, whilst aperturing the high-energy beam will reduce the energy, but also change the confocal parameter. The intensity of the interaction could also be changed without changing the energy, by adjusting the focal position, relative to the target, but beam collimation would also change. The interaction intensity could also be changed by changing the arrival time delay of the pulse relative to that of a target that was moving (such as the electron pulse used in our experiment). Yet, when the target has a duration comparable or even shorter than the laser pulse itself, as is the case in our experiment, then other parameters of the interaction (scattering in our case) will also change (such as the amount of electron charge with which the laser pulse interacts). Ideally, for controlled parametric studies, only a single parameter should be changed at a time, and all others should be kept constant.

We have therefore developed a new method for controlling the energy of the amplified pulse at the output of a high-energy, short-pulse, chirped-pulse-amplified laser system. It relies on the use of a ZHWP to rotate the polarization of the incident laser pulse and the (grating) pulse compressor as the polarizing element. Compared to prior work [23], we find that use of a ZHWP results in negligible spectral modulation as well as minimal distortion due to B-integral effects. By using this method, we can change the pulse energy alone, and keep all other parameters constant, such as the focused spot size and pulse duration. This controlled variation in the output energy is applied to controlling the fluence of X-rays produced by the interaction of a high-power laser pulse with a high-energy laser-driven electron beam.

2. Theoretical model

For the type of laser system discussed in this paper (high-power, ultrashort duration), the large spectral bandwidth of the laser pulse is an important consideration in the performance of the attenuation system because the retardance of the waveplate depends on the wavelength as well as the order. First, we evaluated the wavelength dependent phase retardance for a zero-order waveplate. We compared this with the retardance produced by higher-order waveplates in order to compare the results reported here with prior work that used fifth-order waveplates. The dependence of the phase retardance on wavelength also impacts the polarization state of the output beam—a critical parameter in many applications of high-power laser pulses.

The phase retardance and polarization state are computed using the Jones matrix formulation. For a linear, horizontally polarized beam passing through a general rotated waveplate with phase retardance ϕ and rotation angle θ [24], the electric field of the light after passage through the waveplate, $\boldsymbol{E_T}$, is obtained by application of the corresponding Jones matrix $\boldsymbol{J_{wp}}$ to the incident electric field of the light pulse:

$$\begin{aligned}\boldsymbol{E_T} &= \boldsymbol{J_{wp}}(\boldsymbol{\phi},\theta)\cdot\begin{bmatrix}1\\0\end{bmatrix}\\ &= \begin{bmatrix}\cos\frac{\boldsymbol{\phi}}{2}+\boldsymbol{i}\sin\frac{\boldsymbol{\phi}}{2}\cos 2\boldsymbol{\theta} & \boldsymbol{i}\sin\frac{\boldsymbol{\phi}}{2}\sin 2\boldsymbol{\theta}\\ \boldsymbol{i}\sin\frac{\boldsymbol{\phi}}{2}\sin 2\boldsymbol{\theta} & \cos\frac{\boldsymbol{\phi}}{2}-\boldsymbol{i}\sin\frac{\boldsymbol{\phi}}{2}\cos 2\boldsymbol{\theta}\end{bmatrix}\cdot\begin{bmatrix}1\\0\end{bmatrix}\\ &= \begin{bmatrix}\cos\frac{\boldsymbol{\phi}}{2}+\boldsymbol{i}\sin\frac{\boldsymbol{\phi}}{2}\cos 2\boldsymbol{\theta}\\ \boldsymbol{i}\sin\frac{\boldsymbol{\phi}}{2}\sin 2\boldsymbol{\theta}\end{bmatrix}.\end{aligned} \tag{1}$$

The transmitted light after the waveplate is elliptically polarized in the most general case with a phase shift of $\cos(\boldsymbol{\phi}/2)$. This term is zero for a half-waveplate at the operating wavelength and away from the operating wavelength, this term is non-zero and the magnitude increases with the increase in the order of the waveplate. The phase term contributes to a change of the polarization state of a broadband laser pulse. For $\theta = 45$ deg., corresponding to a rotation of the incident polarization by 90 deg., the ratio of horizontal to vertical polarization can be computed as a function of wavelength. It can be shown that a broadband laser pulse, after passage through a half-waveplate, is no longer linearly polarized and the degree of deviation from this state increases with the increase in the order of the waveplate. For a zero order waveplate, this deviation is small (~1%) for a pulse with 100-nm bandwidth. For a higher order waveplate, this level of deviation is reached for a significantly smaller bandwidth.

The polarizing component of the attenuation system is the gratings in the pulse compressor. For our laser system, these are gold-coated, holographic gratings that have a reflectivity of ~93% for p-polarized light and ~30% for s-polarized light at 800 nm. Since the laser pulse undergoes four reflections in the compressor, the extinction ratio $T_P/T_S = 92.4$. The beam after passage through the ZHWP and grating compressor, in general, is elliptically polarized though the degree of ellipticity is small.

Assuming that the HWP in the energy attenuator is a perfect half-wave plate (PHWP), with rotation angle θ and input energy I_0 for calculation and comparison with the experimental results, the corresponding retardance ϕ equals $\lambda/2$ for a broadband spectrum, so the extra vector disappears. The theoretical P and S polarization energy after the PHWP from Eq. (1), is:

$$I_p = I_o\cos^2(2\theta), \qquad I_s = I_o\sin^2(2\theta) \tag{2}$$

The normalized optimized polarization beam at the exit of the compressor is:

$$I = I_o\cos^2(2\theta) + \frac{I_o\sin^2(2\theta)}{Extinction\ ratio} \tag{3}$$

The beam at the exit of the compressor is linearly polarized with a polarization angle $\mathrm{atan}((\tan^2(2\theta))/95)$, since I_P and I_S in Eq. (2) have the same phase.

3. Experimental results and discussion

We performed two sets of measurements using the 100-terawatt (TW) DIOCLES laser system. First, we experimentally determined the polarization characteristics of the laser pulse after the pulse compressor. This was followed by detailed measurements of the spatial and spectral characteristics. Fig. 1 shows the experimental layout. The laser was operated at the maximum output energy, and the beam was sampled using an attenuation system comprised of a ZHWP, and two TFPs [21], as well as neutral-density filters.

The polarization state of the attenuated high-energy (5 J) pulse from the laser system is purified using a thin film polarizer. This is necessary because the output of the waveplate–polarizer combination is elliptical when the attenuation of the beam is large. When the waveplate is set for maximum transmission, the beam is linearly polarized with a

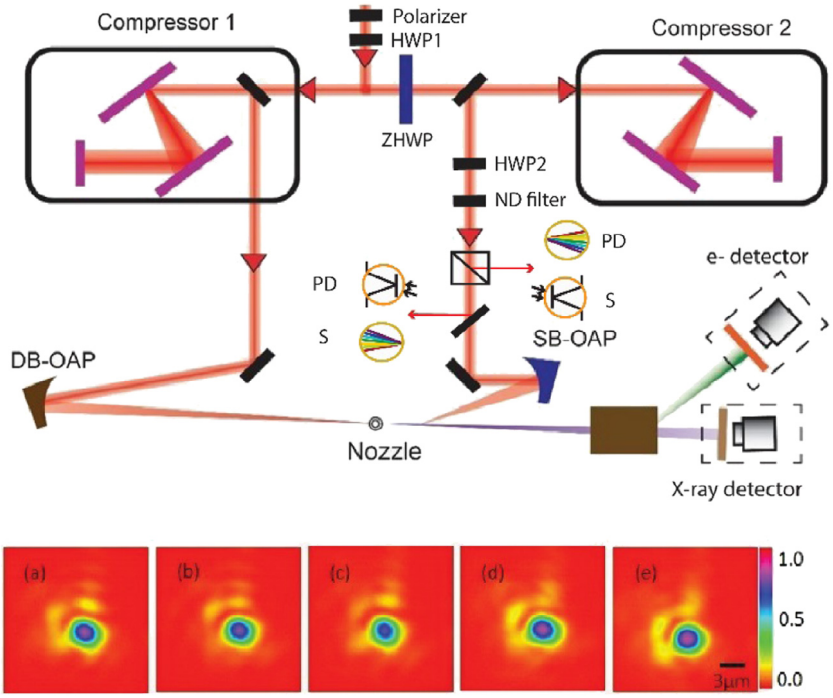

Fig. 1. Layout for continuously attenuating the scattering laser and Inverse-Compton scattering X-rays. The high-energy pulse at the output of the laser system is split in two and compressed using two grating-pulse compressors. The first pulse from compressor 1 is focused by off-axis paraboloid (DB-OAP) and drives the electron beam while the second scattering pulse from compressor 2 is focused (using SB-OAP) and scatters off the laser-driven electron beam to produce X-rays. The energy in the scattering pulse is varied using a compound zero-order half waveplate (ZHWP) located before the compressor. Images of the focal spot produced by SB-OAP for a range of waveplate settings are shown in the bottom panel. Cases (a)–(e) correspond to HWP1 settings shown in Fig. 3. The polarization state of the beam is characterized by low-energy using photodiodes (PD) as shown, but they are removed from the beam path at high power.

polarization ratio of ~200. The polarization state of the laser pulse after the compressor is determined by using HWP2 and a cube polarizer, as shown in Fig. 2. The energy of S and P-polarized beam was measured with a photodiode, and each energy data point was averaged with more than 100 shots. The spectrum without averaging was measured with a spectrometer. Due to the asymmetric response of the broadband cube polarizer used to measure the polarization state of the output beam ($T_p > 90\%$ and $R_s > 99.5\%$), a second half-wave plate (HWP2) is used to obtain maximum reflection into the photodiode to minimize measurement error.

The results of this measurement are shown in Fig. 2 for the attenuation factor, polarization ratio, and the spectral characteristics of the high-energy laser pulse. The measurements shown in Fig. 2(a) indicate that as the half-wave plate at the input of the compressor is rotated, the output energy drops while the polarization ratio degrades. However, for a HWP1 setting of 35 deg., the output energy is attenuated by an order of magnitude, and the polarization ratio is ~10. Beyond this point, the energy is further attenuated; however, the polarization state is no longer linear, and the usefulness of this system is limited. Measurements of the spectrum for a range of half-waveplate angles are shown in Fig. 2(b) and show that the spectrum is nearly invariant with respect to the initial spectrum. Only for a HWP1 setting of 45 deg. is there some loss in spectral width and a corresponding increase in pulse duration. For a HWP1 setting of < 35 deg., the pulse duration remains unchanged. It is to be noted that as the input polarization is rotated, the throughput of the compressor changes on account of the beam being reflected into the non-diffracting zero-order. Independent measurements demonstrate that the sum of the energy in the first-order diffracted beam and the zero-order specular reflection from the grating is constant over the entire range of waveplate settings.

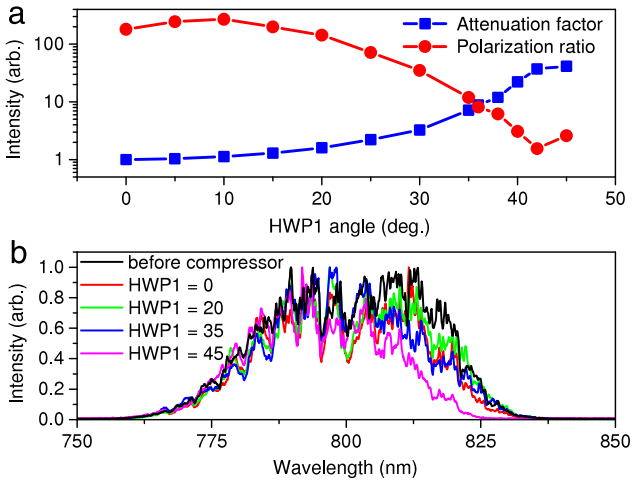

Fig. 2. Measured characteristics of the high-energy attenuation system. (a) Attenuation factor as a function of the angle of HWP1 (blue curve) and corresponding polarization ratio (red curve). (b) Spectrum of the pulse as the waveplate at the input of the pulse compressor is rotated. The spectrum measured at the input of the compressor is also shown for reference. Except for HWP1 = 45 deg., in all other cases, the spectral width is invariant corresponding to a constant pulse duration. (For interpretation of the references to colour in this figure legend, the reader is referred to the web version of this article.)

4. Application for generation of X-rays

We next discuss the application of this novel attenuation system to the generation of X-rays at ultrahigh intensity using the technique of inverse Compton scattering [9]. For this work, the laser operates with maximum output energy of 6 ± 0.3 J at a repetition rate of 0.1 Hz. The high-energy pulse has a temporal duration of 35 fs. The beam is split into two parts before the pulse compressor and independently compressed to deliver two 100-TW laser pulses on target. The layout of the device to generate X-rays is shown in Fig. 3. The first pulse (from compressor 1) is used to generate high-energy electron beams from an underdense plasma by the process of laser wakefield acceleration

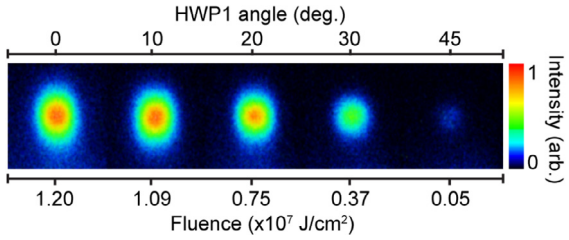

Fig. 3. Controllable X-ray generation using inverse Compton scattering. The X-ray fluence is varied by changing the intensity of the scattering laser pulse using the high-energy attenuation system. Shown are single shot X-ray profiles for a range of laser-fluence. For HWP1 setting of zero, nonlinear effects cause the beam profile to become elliptical. The mean energy of the X-rays shown is 600 keV.

(LWFA). The second pulse scatters off the laser-driven electron beam to produce X-rays.

The energy of the pulse from compressor 2 is varied using the attenuation method already described. The beam is focused using a F#2 optic, and the measured focal spot as a function of the attenuation factor is shown in Fig. 1. The focal spot is optimized using a feedback controlled adaptive optics loop, and it is measured using a high numerical aperture (20X) objective to image the focal plane and recorded on a 12-bit CCD. The measured full-width at half-maximum (FWHM) is $\sim 2.8 \times 2.6$ μm for HWP setting from 0 deg. to 45. deg. The energy enclosed in the FWHM for HWP1 angle 0°is 36.6 ± 1.8%, for 10° is 36.1 ± 1.9%, for 20° is 35.8 ± 1.7%, for 30° is 35.8 ± 1.7%, and for 45° is 36.5 ± 2.9%. The enclosed energy in the focal spot is constant over the entire range of operation.

The results of this experiment are shown in Fig. 3. The electron beam is generated by LWFA using a 2-mm long cylindrical nozzle and a mixed gas target. The mean energy of the electron beam is 170 MeV with a high-energy tail extending out to 300 MeV. The scattering laser pulse then scatters off this beam at a location 2 mm from the exit of the nozzle. The X-rays are detected using a LANEX scintillation screen. The characteristics of the X-ray beam as a function of incident laser fluence are shown in Fig. 3. The results show a monotonic increase in the X-ray fluence as the energy in the scattering beam is increased. For lower intensities, the X-ray profile is determined by linear scattering processes, and the mean energy is ~600 keV. At the highest laser fluence, the X-ray profile is slightly elliptical, and the photon energy is red-shifted by a factor of two due to nonlinear effects [18]. We have thus demonstrated a system to control the characteristics of Thomson X-rays by varying the energy in the scattering laser pulse.

5. Conclusions

In conclusion, we report a novel system to control the energy of a high-power, short-pulse laser system. The method is simple, robust, and preserves the spectral and spatial characteristics of the laser pulse. The attenuation factor is an order of magnitude while keeping the polarization ratio > 10. This can be further increased by a factor of two or more with the latest gratings that achieve reflectivity $> 95\%$ for p-polarization. This method can also be used for much shorter pulses < 20 fs making it possible to implement on short-pulse, PW-peak-power systems. Implementation of this system in a compact all-laser-driven Thomson X-ray light source allowed us to control the output X-ray dose in steps that could be arbitrarily small, over a large intensity range. It is also applicable to control and study any processes that depend on laser intensity. In particular, the technique is anticipated to be critical to the success of current and future high field physics experiments, such as studies of nonlinear scattering, radiation-reaction force and quantum electrodynamic effects [18] where on account of the nonlinearity of the process, the intensity dependence provides accurate signatures for the physical process under study.

Acknowledgments

We thank Kevin Brown and Jared Mills for operating the laser system, and Chad Petersen for data acquisition.

Funding

This material is based upon work supported by National Science Foundation under Grant No. PHY-1535700 (ultra-low emittance electron beams); the US Department of Energy (DOE), Office of Science, Basic Energy Sciences (BES), under Award # DE-FG02-05ER15663 (laser-driven X-rays for ultrafast science); the Air Force Office for Scientific Research under award number FA9550-14-1-0345 (interactions of electrons with laser light at highly relativistic intensities); and the U.S. Department of Homeland Security Domestic Nuclear Detection Office, under competitively awarded contract HSHQDC-13-C-B0036 (low-dose X-ray radiography). This support does not constitute an express or implied endorsement on the part of the Government.

References

[1] D. Strickland, G. Mourou, Compression of amplified chirped optical pulses, Opt. Commun. 56 (1985) 219–221.
[2] I. Ross, P. Matousek, M. Towrie, A. Langley, J. Collier, The prospects for ultrashort pulse duration and ultrahigh intensity using optical parametric chirped pulse amplifiers, Opt. Commun. 144 (1997) 125–133.
[3] F. Ple, M. Pittman, G. Jamelot, J. Chambaret, Design and demonstration of a high-energy booster amplifier for a high-repetition rate petawatt class laser system, Opt. Lett. 32 (2007) 238–240.
[4] V. Lozhkarev, G. Freidman, V. Ginzburg, E. Katin, E. Khazanov, A. Kirsanov, G. Luchinin, A. Mal'Shakov, M. Martyanov, O. Palashov, Compact 0.56 petawatt laser system based on optical parametric chirped pulse amplification in KD* P crystals, Laser Phys. Lett. 4 (2007) 421.
[5] L. Xu, L. Yu, X. Liang, Y. Chu, Z. Hu, L. Ma, Y. Xu, C. Wang, X. Lu, H. Lu, High-energy noncollinear optical parametric–chirped pulse amplification in LBO at 800 nm, Opt. Lett. 38 (2013) 4837–4840.
[6] Z. Wang, C. Liu, Z. Shen, Q. Zhang, H. Teng, Z. Wei, High-contrast 1.16 PW Ti: Sapphire laser system combined with a doubled chirped-pulse amplification scheme and a femtosecond optical-parametric amplifier, Opt. Lett. 36 (2011) 3194–3196.
[7] Y. Chu, Z. Gan, X. Liang, L. Yu, X. Lu, C. Wang, X. Wang, L. Xu, H. Lu, D. Yin, High-energy large-aperture Ti: Sapphire amplifier for 5 PW laser pulses, Opt. Lett. 40 (2015) 5011–5014.
[8] T.J. Yu, S.K. Lee, J.H. Sung, J.W. Yoon, T.M. Jeong, J. Lee, Generation of high-contrast, 30 fs, 1.5 PW laser pulses from chirped-pulse amplification Ti: Sapphire laser, Opt. Express 20 (2012) 10807–10815.
[9] D.P. Umstadter, All-laser-driven Thomson X-ray sources, Contemp. Phys. 56 (2015) 417–431.
[10] E. Esarey, C. Schroeder, W. Leemans, Physics of laser-driven plasma-based electron accelerators, Rev. Modern Phys. 81 (2009) 1229.
[11] W. Leemans, A. Gonsalves, H. Mao, K. Nakamura, C. Benedetti, C. Schroeder, C. Tóth, J. Daniels, D. Mittelberger, S. Bulanov, Multi-GeV electron beams from capillary-discharge-guided subpetawatt laser pulses in the self-trapping regime, Phys. Rev. Lett. 113 (2014) 245002.
[12] S. Chen, N.D. Powers, I. Ghebregziabher, C.M. Maharjan, C. Liu, G. Golovin, S. Banerjee, J. Zhang, N. Cunningham, A. Moorti, S. Clarke, S. Pozzi, D.P. Umstadter, MeV-energy X rays from inverse compton scattering with laser-wakefield accelerated electrons, Phys. Rev. Lett. 110 (2013) 155003.
[13] N.D. Powers, I. Ghebregziabher, G. Golovin, C. Liu, S. Chen, S. Banerjee, J. Zhang, D.P. Umstadter, Quasi-monoenergetic and tunable X-rays from a laser-driven Compton light source, Nat. Photonics 8 (2014) 28–31.
[14] A. Macchi, M. Borghesi, M. Passoni, Ion acceleration by superintense laser-plasma interaction, Rev. Modern Phys. 85 (2013) 751.
[15] V. Malka, J. Faure, Y.A. Gauduel, E. Lefebvre, A. Rousse, K.T. Phuoc, Principles and applications of compact laser–plasma accelerators, Nat. Phys. 4 (2008) 447–453.
[16] S.W. Bahk, P. Rousseau, T.A. Planchon, V. Chvykov, G. Kalintchenko, A. Maksimchuk, G.A. Mourou, V. Yanovsky, Generation and characterization of the highest laser intensities (10(22) W/cm(2)), Opt. Lett. 29 (2004) 2837.
[17] B. Zhao, J. Zhang, S. Chen, C. Liu, G. Golovin, S. Banerjee, K. Brown, J. Mills, C. Petersen, D. Umstadter, Wavefront-correction for nearly diffraction-limited focusing of dual-color laser beams to high intensities, Opt. Express 22 (2014) 26947–26955.
[18] A. Di Piazza, C. Mueller, K.Z. Hatsagortsyan, C.H. Keitel, Extremely high-intensity laser interactions with fundamental quantum systems, Rev. Modern Phys. 84 (2012) 1177–1228.
[19] L. Robson, P.T. Simpson, R.J. Clarke, K.W.D. Ledingham, F. Lindau, O. Lundh, T. McCanny, P. Mora, D. Neely, C.-. Wahlstrom, M. Zepf, P. McKenna, Scaling of proton acceleration driven by petawatt-laser-plasma interactions, Nat. Phys. 3 (2007) 58–62.

[20] K. Yamakawa, Y. Akahane, Y. Fukuda, M. Aoyama, N. Inoue, H. Ueda, T. Utsumi, Many-Electron dynamics of a Xe atom in strong and superstrong laser fields, Phys. Rev. Lett. 92 (2004) 123001.
[21] C. Liu, J. Zhang, S. Chen, G. Golovin, S. Banerjee, B. Zhao, N. Powers, I. Ghebregziabher, D. Umstadter, Adaptive-feedback spectral-phase control for interactions with transform-limited ultrashort high-power laser pulses, Opt. Lett. 39 (2014) 80–83.
[22] D.M.A. Aminou, J. Squier, Broad band thin film plate polarizer for high power femtosecond solid-state lasers, Adv. Solid State Lasers 15 (1993) 212–215.
[23] Y. Zhao, Y. Jia, J. Yang, X. Zhu, Influence of a half-wave plate–polarizer attenuator on broadband femtosecond laser pulses, Opt. Eng. 46 (2007) 044301.
[24] E. Collett, Field Guide To Polarization, SPIE Press, Bellingham, WA, 2005.